A&A 408, 1197–1203 (2003)
DOI: 10.1051/0004-6361:20030969

Astronomy & Astrophysics

Collisional excitation rates of H_2O with H_2

II. Rotational excitation with ortho-H_2 at very low temperature and application to cold molecular clouds

A. Grosjean[1], M.-L. Dubernet[2], and C. Ceccarelli[3]

[1] Laboratoire d'Astrophysique, UMR CNRS 6091, Observatoire de Besançon, Université de Franche-Comté, 41 bis avenue de l'Observatoire, BP 1615, 25010 Besançon Cedex, France
[2] LERMA FRE 2460, Observatoire de Paris, Section de Meudon, 5 place Janssen, 92195 Meudon Cedex, France
[3] Laboratoire d'Astrophysique de l'Observatoire de Grenoble, 414 rue de la Piscine, BP 53, 38041 Grenoble Cedex 9, France

Received 13 March 2003 / Accepted 12 June 2003

Abstract. We present the results of close coupling calculations of pure rotational excitation rate coefficients of H_2O by ortho-H_2, performed between 5 K and 20 K. At 20 K there is a good agreement with those results obtained previously by Phillips et al. (1996). Fits of our de-excitation collisional rate coefficients are provided. These new rate coefficients are used in the modelling of cold interstellar clouds to determine the influence of the precision of the rate coefficients on predicted line intensities.

Key words. molecular data – molecular processes – ISM: molecules

1. Introduction

Water is a key molecule for the chemistry and the energy balance of the gas in cold clouds and star forming regions, thanks to its relatively large abundance and large dipole moment. For a long time chemical models have predicted the water abundance to be around 10^{-7} in cold clouds (Lee et al. 1996), i.e. among the most abundant O-bearing molecules. Yet, in warm regions water is expected to become the main reservoir of oxygen, thanks to both evaporation of the icy grain mantles (Tielens & Allamandola 1987b,a) and endothermic reactions that transform all the gaseous oxygen not in CO but rather into H_2O (Graff & Dalgarno 1987). Heating of the gas occurs both because of the absorption of the radiation emitted by a newly born star (Ceccarelli et al. 1996; Doty & Neufeld 1997), and because of the strong molecular shocks emanating from the protostar itself (Kaufman & Neufeld 1996a,b). For this reason, water modeling deserves particular attention. In this respect, collisional rotational and ro-vibrational excitation rates of H_2O by H_2 are essential for the interpretation of excitation conditions and for the determination of chemical composition in the different media.

This paper is the second part of a thorough theoretical study of the collisional excitation rates of H_2O by H_2. The study is motivated both by the intepretation of the data recently acquired by the *Infrared Space Observatory* (Kessler et al. 1996) and the *Submillimeter Wave Astronomy Satellite* (hereinafter SWAS; Melnick et al. 2000), and by the future ESA mission, the Herschel Space Observatory (hereinafter HSO). Specifically, the Heterodyne Instrument for the Far-Infrared on board HSO will allow observations of several water lines with unprecedented sensitivity in different environments, from the interstellar medium to stellar or planetary atmospheres.

In Paper I Dubernet & Grosjean (2002) calculated the pure rotational (de)-excitation rate coefficients of ortho/para H_2O by para H_2 at very low temperatures ($T \leq 20$ K). The other available excitation rate coefficients of H_2O by H_2 are those calculated by Phillips et al. (1995, 1996), using the close-coupling and the coupled states methods with a potential energy surface (PES) calculated by Phillips et al. (1994). Those authors provided data between 20 K and 140 K for a number of ortho/para H_2O – ortho/para H_2 pure rotational transitions. The results presented in Paper I (Dubernet & Grosjean 2002) were significantly different from those presented earlier by Phillips et al. (1996) at 20 K. In particular, the excitation rate coefficient for the 1_{01}–1_{10} transition of water was more than 50% larger than the Phillips et al. (1996) result. This was a consequence of an inadequately fine energy grid used by Phillips et al. (1996) in integrating the cross-sections over a Maxwellian distribution of kinetic energies.

An analysis of the results of Paper I (Dubernet & Grosjean 2002) shows that reasonable extrapolation of the high temperature data gives up to 50% error at 5 K for the 1_{01}–1_{10} transition of water. By reasonable extrapolation, we mean using a power law fit for the de-excitation rate coefficients of the 1_{01}–1_{10} transition, with our calculated points at 16 K and 20 K, and obtaining the excitation rate coefficients by detailed balance.

Send offprint requests to: M.-L. Dubernet,
e-mail: marie-lise.dubernet@obspm.fr

Table 1. Propagation parameters of MOLSCAT used in our calculations (see the MOLSCAT documentation, Hutson & Green 1994, for the meaning of the parameters).

Propagation parameters		
INTFLG = 6	STEPS = 10	
DTOL = 0.3	OTOL = 0.005	
RMIN = 1 (adjusted)	IRMSET = 0	RMAX = 50 (adjusted)

This type of extrapolation may be justified because of the low dependence of the de-excitation rate coefficients on temperature.

Both the differences found with earlier results of Phillips et al. (1996) and the inadequacy of rate coefficient extrapolation in the particular case of Paper I (Dubernet & Grosjean 2002) motivated the present determination of pure rotational excitation rate coefficients of ortho/para H_2O by ortho H_2 at very low temperatures ($T \leq 20$ K) where no data have yet been calculated. We use the same PES (Phillips et al. 1994) and the same description of the water molecule as Phillips et al. (1995), which allows us to compare the collision rate coefficients we obtain at 20 K with those of Phillips et al. (1995, 1996). However we use improved dynamical calculations compared to the earlier calculations of Phillips et al. (1996). This implies using a larger rotational basis set, a finer energy grid and close coupling calculations on the whole energy range. The description of the quantum calculation and the analysis of the rotational excitation rate coefficients are given in Sect. 2.

Section 3 investigates the use of rate coefficients in a specific LVG model of cold interstellar clouds, in order to provide a simple test of the influence of the precision of rate coefficients on the predicted water line intensities.

2. Methods and rate coefficients

Close coupling calculations are done in the same spirit as in Paper I (Dubernet & Grosjean 2002): we use Green's code of the PES of Phillips et al. (1994) and the MOLSCAT (Hutson & Green 1994) code with correctly converged parameters (see Table 1). The water molecule is described by a version of the effective Hamiltonian of Kyrö (1981), compatible with the symmetries of the PES. We use the molecular constants of Table I of Kyrö (1981) and our calculated rotational levels of $H_2^{16}O$ are identical to those of Green et al. (1993). The reduced mass of the system is 1.81277373 a.m.u. and the hydrogen molecule is taken as a rigid rotor with a rotational constant of 60.853 cm^{-1}.

The state-to-state rotational inelastic rate coefficients are the Boltzmann thermal averages of the inelastic cross sections:

$$R(\beta \rightarrow \beta')(T) = \left(\frac{8}{\pi\mu}\right)^{1/2} \frac{1}{(kT)^{3/2}} \times \int_0^\infty \sigma_{\beta\rightarrow\beta'}(E) E \mathrm{e}^{-E/kT} \mathrm{d}E, \quad (1)$$

where $\beta \equiv j\alpha$, j_2 and $\beta' \equiv j'\alpha'$, j_2', unprimed and primed quantum numbers label initial and final states of the molecules, j and j_2 are the rotational angular momenta of H_2O and H_2 and α specifies the other H_2O quantum numbers (e.g. K_{-1}, K_1), E is the kinetic energy and k is the Boltzmann constant. The rate coefficients are obtained using an analytical integration for temperatures ranging from 5 K to 20 K, the inelastic cross sections being interpolated by straight lines between calculated values. Calculations are made over essentially the whole energy range spanned by the Boltzmann distributions; the highest energy point calculated is at the threshold energy of the transition plus $10kT$.

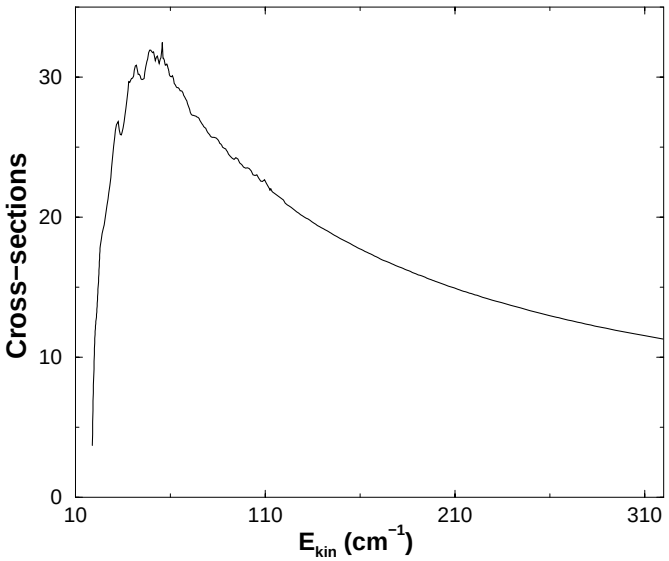

Fig. 1. Inelastic cross-section (in Å^2) as a function of kinetic energy (in cm^{-1}) of the water $1_{0,1} \rightarrow 1_{1,0}$ transition (with $j_2 = 1$).

We carefully spanned the energy ranges above the inelastic channels and added more points in the presence of resonance structures. We found that the resonances do not play an important role once the cross-sections are averaged over energy, contrary to what was found for the excitation of water by para-H_2 (Dubernet & Grosjean 2002). This is due to the large magnitude of the excitation cross-sections of water by ortho-H_2, compared to the magnitude of the resonance structures, as is shown in Fig. 1. The energy grid used is therefore sparser than for para-H_2, but still much finer than the one used by Phillips et al. (1996).

The effective rotational inelastic rate coefficients are given by the sum of the inelastic rate coefficients (Eq. (1)) over the final j_2' states for a given initial j_2:

$$\hat{R}_{j_2=1}(j\alpha \rightarrow j'\alpha')(T) = \sum_{j_2'} R(j\alpha, j_2 = 1 \rightarrow j'\alpha', j_2')(T). \quad (2)$$

In the temperature range between 5 K and 20 K, the inelastic rate coefficients from transitions between $j_2 = 1$ and $j_2' = 3$ are zero.

For collisions of H_2O with ortho-H_2, Phillips et al. (1996) concluded that a $B(j_1 = 5, j_2 = 1)$ basis set is sufficient for obtaining an accuracy of better than 10% in the temperature range from 20 K to 140 K; it is not necessary to use a $B(j_1 = 5, j_2 = 3)$ basis set (the values of j_1 and j_2 indicated are the maximum rotational quantum numbers of H_2O

Table 2. Effective rate coefficients of Eq. (2) (in $cm^3\ s^{-1}$) of ortho-H_2O with ortho-H_2 ($j_2 = 1$). The levels are labelled with $j_{K_{-1}K_1}$. The column "Points" gives the number of energy points used in the Boltzmann average. The last column gives the data of Phillips et al. (1996). The levels are organized according to increasing energy as in the paper of Phillips et al. (1996).

Initial	Final	Points	5	8	12	16	20	20
$1_{0,1}$	$1_{1,0}$	396	1.04(E-12)	8.24(E-12)	2.68(E-11)	4.91(E-11)	7.10(E-11)	7.04(E-11)
$1_{0,1}$	$2_{1,2}$	288	1.41(E-17)	6.13(E-15)	1.87(E-13)	1.05(E-12)	3.01(E-12)	2.94(E-12)
$1_{0,1}$	$2_{2,1}$	171	4.54(E-25)	7.38(E-20)	5.90(E-17)	1.69(E-15)	1.27(E-14)	1.20(E-14)
$1_{0,1}$	$3_{0,3}$	161	3.37(E-25)	6.62(E-20)	5.87(E-17)	1.76(E-15)	1.36(E-14)	1.16(E-14)
$1_{0,1}$	$3_{1,2}$	120	1.85(E-30)	2.08(E-23)	1.78(E-19)	1.66(E-17)	2.54(E-16)	2.31(E-16)
$1_{0,1}$	$3_{2,1}$	86	2.08(E-35)	1.47(E-26)	1.24(E-21)	3.63(E-19)	1.11(E-17)	1.11(E-17)
$1_{0,1}$	$4_{1,4}$	68	6.68(E-37)	1.79(E-27)	3.10(E-22)	1.28(E-19)	4.78(E-18)	5.89(E-18)
$1_{0,1}$	$3_{3,0}$	40	4.59(E-45)	8.64(E-33)	5.70(E-26)	1.46(E-22)	1.63(E-20)	1.58(E-20)
$1_{0,1}$	$4_{2,3}$	33	3.23(E-47)	3.14(E-34)	5.10(E-27)	2.03(E-23)	2.92(E-21)	3.27(E-21)
$1_{1,0}$	$1_{0,1}$	396	2.18(E-10)	2.33(E-10)	2.49(E-10)	2.61(E-10)	2.70(E-10)	2.68(E-10)
$1_{1,0}$	$2_{1,2}$	288	3.29(E-15)	1.90(E-13)	1.86(E-12)	5.87(E-12)	1.17(E-11)	1.11(E-11)
$1_{1,0}$	$2_{2,1}$	171	2.25(E-22)	4.98(E-18)	1.32(E-15)	2.16(E-14)	1.17(E-13)	1.16(E-13)
$1_{1,0}$	$3_{0,3}$	161	6.65(E-23)	1.73(E-18)	4.93(E-16)	8.30(E-15)	4.50(E-14)	4.44(E-14)
$1_{1,0}$	$3_{1,2}$	120	7.45(E-28)	1.12(E-21)	3.13(E-18)	1.69(E-16)	1.87(E-15)	1.80(E-15)
$1_{1,0}$	$3_{2,1}$	86	3.20(E-33)	3.00(E-25)	8.07(E-21)	1.34(E-18)	2.89(E-17)	2.60(E-17)
$1_{1,0}$	$4_{1,4}$	68	1.12(E-34)	4.17(E-26)	2.41(E-21)	5.79(E-19)	1.55(E-17)	1.70(E-17)
$1_{1,0}$	$3_{3,0}$	40	3.69(E-42)	9.39(E-31)	2.04(E-24)	3.00(E-21)	2.39(E-19)	2.37(E-19)
$1_{1,0}$	$4_{2,3}$	33	1.69(E-44)	2.23(E-32)	1.21(E-25)	2.83(E-22)	2.98(E-20)	3.64(E-20)
$2_{1,2}$	$1_{0,1}$	288	7.68(E-11)	8.22(E-11)	8.89(E-11)	9.46(E-11)	9.93(E-11)	9.71(E-11)
$2_{1,2}$	$1_{1,0}$	288	8.52(E-11)	9.02(E-11)	9.55(E-11)	9.90(E-11)	1.01(E-10)	9.67(E-11)
$2_{1,2}$	$2_{2,1}$	171	8.13(E-18)	3.46(E-15)	1.03(E-13)	5.67(E-13)	1.59(E-12)	1.52(E-12)
$2_{1,2}$	$3_{0,3}$	161	6.79(E-18)	3.46(E-15)	1.15(E-13)	6.75(E-13)	1.97(E-12)	1.91(E-12)
$2_{1,2}$	$3_{1,2}$	120	1.09(E-22)	2.95(E-18)	8.76(E-16)	1.53(E-14)	8.51(E-14)	7.92(E-14)
$2_{1,2}$	$3_{2,1}$	86	6.73(E-28)	1.18(E-21)	3.53(E-18)	1.95(E-16)	2.18(E-15)	2.11(E-15)
$2_{1,2}$	$4_{1,4}$	68	1.18(E-29)	8.19(E-23)	5.24(E-19)	4.22(E-17)	5.91(E-16)	5.34(E-16)
$2_{1,2}$	$3_{3,0}$	40	8.15(E-38)	3.90(E-28)	9.39(E-23)	4.62(E-20)	1.91(E-18)	1.77(E-18)
$2_{1,2}$	$4_{2,3}$	33	1.13(E-39)	2.54(E-29)	1.42(E-23)	1.04(E-20)	5.45(E-19)	5.54(E-19)
$2_{2,1}$	$1_{0,1}$	171	2.03(E-11)	2.08(E-11)	2.15(E-11)	2.20(E-11)	2.25(E-11)	2.15(E-11)
$2_{2,1}$	$1_{1,0}$	171	4.82(E-11)	4.98(E-11)	5.16(E-11)	5.31(E-11)	5.43(E-11)	5.42(E-11)
$2_{2,1}$	$2_{1,2}$	171	6.69(E-11)	7.29(E-11)	7.85(E-11)	8.25(E-11)	8.54(E-11)	8.19(E-11)
$2_{2,1}$	$3_{0,3}$	161	2.34(E-11)	3.21(E-11)	3.98(E-11)	4.45(E-11)	4.72(E-11)	4.48(E-11)
$2_{2,1}$	$3_{1,2}$	120	7.14(E-16)	5.18(E-14)	5.88(E-13)	2.02(E-12)	4.26(E-12)	3.95(E-12)
$2_{2,1}$	$3_{2,1}$	86	1.00(E-20)	4.65(E-17)	5.22(E-15)	5.66(E-14)	2.40(E-13)	2.31(E-13)
$2_{2,1}$	$4_{1,4}$	68	4.92(E-23)	8.56(E-19)	1.97(E-16)	3.01(E-15)	1.56(E-14)	1.60(E-14)
$2_{2,1}$	$3_{3,0}$	40	7.28(E-30)	8.68(E-23)	7.43(E-19)	6.89(E-17)	1.04(E-15)	1.03(E-15)
$2_{2,1}$	$4_{2,3}$	33	1.52(E-32)	9.75(E-25)	2.15(E-20)	3.22(E-18)	6.52(E-17)	5.24(E-17)
$3_{0,3}$	$1_{0,1}$	161	1.90(E-11)	1.90(E-11)	1.92(E-11)	1.95(E-11)	1.98(E-11)	1.69(E-11)
$3_{0,3}$	$1_{1,0}$	161	1.79(E-11)	1.76(E-11)	1.74(E-11)	1.73(E-11)	1.72(E-11)	1.70(E-11)
$3_{0,3}$	$2_{1,2}$	161	6.98(E-11)	7.37(E-11)	7.89(E-11)	8.32(E-11)	8.66(E-11)	8.40(E-11)
$3_{0,3}$	$2_{2,1}$	161	2.86(E-11)	3.21(E-11)	3.56(E-11)	3.76(E-11)	3.86(E-11)	3.66(E-11)
$3_{0,3}$	$3_{1,2}$	120	3.60(E-15)	2.05(E-13)	2.00(E-12)	6.34(E-12)	1.28(E-11)	1.28(E-11)
$3_{0,3}$	$3_{2,1}$	86	8.57(E-21)	3.09(E-17)	2.92(E-15)	2.83(E-14)	1.10(E-13)	1.02(E-13)
$3_{0,3}$	$4_{1,4}$	68	5.61(E-22)	8.19(E-18)	1.73(E-15)	2.55(E-14)	1.29(E-13)	1.23(E-13)
$3_{0,3}$	$3_{3,0}$	40	1.13(E-30)	1.03(E-23)	7.27(E-20)	5.91(E-18)	8.11(E-17)	9.21(E-17)
$3_{0,3}$	$4_{2,3}$	33	5.84(E-32)	2.95(E-24)	5.67(E-20)	7.90(E-18)	1.53(E-16)	1.39(E-16)

and H_2 used included in the basis). We performed close coupling calculations with both $B(5, 1)$ and $B(5, 3)$ basis sets in the energy range from the opening of the lowest inelastic channel to a total energy of $750\,cm^{-1}$. The corresponding effective rate coefficients have absolute relative differences ranging from 2% to 30%, the $B(5, 3)$ rate coefficients being generally but not always larger than $B(5, 1)$ rates. The biggest differences correspond to the smallest rate coefficients. Tables 2 and 3 give the effective rotational inelastic rate coefficients at several temperature calculated with a $B(5, 3)$ basis set, for ortho and para H_2O respectively, together with the values obtained by Phillips et al. (1995) at 20 K with a $B(5, 1)$ basis set.

Table 3. Effective rate coefficients of Eq. (2) (in $cm^3\ s^{-1}$) of para-H_2O with ortho-H_2 ($j_2 = 1$). The levels are labelled with $j_{K_{-1}K_1}$. The column "Points" gives the number of energy points used in the Boltzmann average. The last column gives the data of Phillips et al. (1996). The levels are organized according to increasing energy as in the paper of Phillips et al. (1996).

Initial	Final	Points	5	8	12	16	20	20
$0_{0,0}$	$1_{1,1}$	326	6.02(E-15)	3.54(E-13)	3.48(E-12)	1.10(E-11)	2.22(E-11)	2.19(E-11)
$0_{0,0}$	$2_{0,2}$	259	2.22(E-19)	4.40(E-16)	3.04(E-14)	2.54(E-13)	9.14(E-13)	8.31(E-13)
$0_{0,0}$	$2_{1,1}$	209	3.15(E-23)	1.03(E-18)	3.48(E-16)	6.46(E-15)	3.73(E-14)	3.36(E-14)
$0_{0,0}$	$2_{2,0}$	135	3.13(E-28)	7.60(E-22)	2.72(E-18)	1.65(E-16)	1.96(E-15)	1.90(E-15)
$0_{0,0}$	$3_{1,3}$	120	2.49(E-29)	1.14(E-22)	5.79(E-19)	4.15(E-17)	5.40(E-16)	6.30(E-16)
$0_{0,0}$	$3_{2,2}$	87	2.99(E-38)	1.53(E-28)	3.62(E-23)	1.68(E-20)	6.51(E-19)	7.48(E-19)
$0_{0,0}$	$4_{0,4}$	65	1.40(E-39)	3.69(E-29)	2.29(E-23)	1.82(E-20)	1.00(E-18)	9.90(E-19)
$0_{0,0}$	$4_{1,3}$	51	6.97(E-47)	6.09(E-34)	9.58(E-27)	3.82(E-23)	5.51(E-21)	5.69(E-21)
$0_{0,0}$	$3_{3,1}$	42	6.26(E-48)	1.47(E-34)	3.97(E-27)	2.07(E-23)	3.51(E-21)	3.13(E-21)
$1_{1,1}$	$0_{0,0}$	326	8.82(E-11)	9.42(E-11)	9.96(E-11)	1.04(E-10)	1.07(E-10)	1.06(E-10)
$1_{1,1}$	$2_{0,2}$	259	1.74(E-14)	6.52(E-13)	5.00(E-12)	1.39(E-11)	2.56(E-11)	2.51(E-11)
$1_{1,1}$	$2_{1,1}$	209	6.25(E-18)	3.61(E-15)	1.29(E-13)	7.86(E-13)	2.34(E-12)	2.27(E-12)
$1_{1,1}$	$2_{2,0}$	135	2.77(E-23)	1.24(E-18)	4.83(E-16)	9.63(E-15)	5.86(E-14)	5.73(E-14)
$1_{1,1}$	$3_{1,3}$	120	2.84(E-24)	2.45(E-19)	1.37(E-16)	3.26(E-15)	2.19(E-14)	1.99(E-14)
$1_{1,1}$	$3_{2,2}$	87	5.60(E-33)	5.09(E-25)	1.33(E-20)	2.15(E-18)	4.52(E-17)	4.93(E-17)
$1_{1,1}$	$4_{0,4}$	65	8.49(E-35)	3.85(E-26)	2.48(E-21)	6.31(E-19)	1.75(E-17)	1.95(E-17)
$1_{1,1}$	$4_{1,3}$	51	4.41(E-42)	6.93(E-31)	1.15(E-24)	1.48(E-21)	1.08(E-19)	1.00(E-19)
$1_{1,1}$	$3_{3,1}$	42	7.56(E-43)	3.26(E-31)	9.51(E-25)	1.63(E-21)	1.43(E-19)	1.29(E-19)
$2_{0,2}$	$0_{0,0}$	259	2.59(E-11)	2.64(E-11)	2.72(E-11)	2.78(E-11)	2.83(E-11)	2.58(E-11)
$2_{0,2}$	$1_{1,1}$	259	1.39(E-10)	1.48(E-10)	1.56(E-10)	1.62(E-10)	1.65(E-10)	1.61(E-10)
$2_{0,2}$	$2_{1,1}$	209	1.25(E-13)	1.99(E-12)	9.54(E-12)	2.12(E-11)	3.45(E-11)	3.49(E-11)
$2_{0,2}$	$2_{2,0}$	135	1.61(E-19)	2.01(E-16)	1.05(E-14)	7.63(E-14)	2.51(E-13)	2.35(E-13)
$2_{0,2}$	$3_{1,3}$	120	7.72(E-20)	1.99(E-16)	1.63(E-14)	1.50(E-13)	5.73(E-13)	5.52(E-13)
$2_{0,2}$	$3_{2,2}$	87	1.93(E-28)	5.26(E-22)	2.00(E-18)	1.23(E-16)	1.47(E-15)	1.45(E-15)
$2_{0,2}$	$4_{0,4}$	65	1.84(E-30)	2.48(E-23)	2.31(E-19)	2.25(E-17)	3.53(E-16)	3.09(E-16)
$2_{0,2}$	$4_{1,3}$	51	7.54(E-38)	3.51(E-28)	8.52(E-23)	4.25(E-20)	1.77(E-18)	1.51(E-18)
$2_{0,2}$	$3_{3,1}$	42	2.89(E-39)	3.58(E-29)	1.46(E-23)	9.28(E-21)	4.46(E-19)	4.04(E-19)
$2_{1,1}$	$0_{0,0}$	209	5.00(E-12)	5.63(E-12)	6.31(E-12)	6.75(E-12)	7.02(E-12)	6.35(E-12)
$2_{1,1}$	$1_{1,1}$	209	6.84(E-11)	7.47(E-11)	8.18(E-11)	8.74(E-11)	9.16(E-11)	8.88(E-11)
$2_{1,1}$	$2_{0,2}$	209	1.73(E-10)	1.82(E-10)	1.94(E-10)	2.03(E-10)	2.10(E-10)	2.12(E-10)
$2_{1,1}$	$2_{2,0}$	135	8.60(E-16)	7.72(E-14)	9.66(E-13)	3.47(E-12)	7.51(E-12)	7.45(E-12)
$2_{1,1}$	$3_{1,3}$	120	8.30(E-17)	1.40(E-14)	2.46(E-13)	1.04(E-12)	2.48(E-12)	2.35(E-12)
$2_{1,1}$	$3_{2,2}$	87	4.20(E-25)	7.62(E-20)	6.45(E-17)	1.89(E-15)	1.44(E-14)	1.45(E-14)
$2_{1,1}$	$4_{0,4}$	65	1.78(E-27)	1.59(E-21)	3.25(E-18)	1.49(E-16)	1.48(E-15)	1.49(E-15)
$2_{1,1}$	$4_{1,3}$	51	2.60(E-34)	7.99(E-26)	4.22(E-21)	9.81(E-19)	2.60(E-17)	2.32(E-17)
$2_{1,1}$	$3_{3,1}$	42	1.30(E-35)	1.09(E-26)	9.98(E-22)	3.04(E-19)	9.44(E-18)	8.05(E-18)
$2_{2,0}$	$0_{0,0}$	135	6.97(E-12)	6.82(E-12)	6.84(E-12)	6.95(E-12)	7.10(E-12)	6.86(E-12)
$2_{2,0}$	$1_{1,1}$	135	4.21(E-11)	4.18(E-11)	4.23(E-11)	4.31(E-11)	4.40(E-11)	4.28(E-11)
$2_{2,0}$	$2_{0,2}$	135	3.06(E-11)	2.99(E-11)	2.95(E-11)	2.93(E-11)	2.93(E-11)	2.73(E-11)
$2_{2,0}$	$2_{1,1}$	135	1.19(E-10)	1.26(E-10)	1.33(E-10)	1.39(E-10)	1.44(E-10)	1.42(E-10)
$2_{2,0}$	$3_{1,3}$	120	8.03(E-12)	1.60(E-11)	2.35(E-11)	2.84(E-11)	3.18(E-11)	3.11(E-11)
$2_{2,0}$	$3_{2,2}$	87	7.97(E-20)	1.82(E-16)	1.38(E-14)	1.22(E-13)	4.54(E-13)	4.68(E-13)
$2_{2,0}$	$4_{0,4}$	65	1.27(E-22)	1.40(E-18)	2.58(E-16)	3.62(E-15)	1.78(E-14)	1.77(E-14)
$2_{2,0}$	$4_{1,3}$	51	5.39(E-29)	1.91(E-22)	8.22(E-19)	5.34(E-17)	6.51(E-16)	6.29(E-16)
$2_{2,0}$	$3_{3,1}$	42	1.19(E-29)	1.19(E-22)	9.21(E-19)	8.13(E-17)	1.20(E-15)	1.09(E-15)

Table 4. Coefficients $a^{(n)}_{j_2=1;j\alpha\leftarrow j'\alpha'}$ (n = 0 to 4) of the polynomial fit (Eq. (3)) to the effective de-excitation rate coefficients of ortho-water in Table 2. The effective excitation rate coefficients can be obtained by detailed balance. The first column gives the final state and the polynomial order n, the following columns give the fitting coefficients for various initial states. The levels are labelled with $j_{K_{-1}K_1}$. We emphasize that these fits are only valid in the temperature range from 5 K to 20 K.

$1_{0,1}$	$a^{(n)}_{\leftarrow 1_{1,0}}$	$a^{(n)}_{\leftarrow 2_{1,2}}$	$a^{(n)}_{\leftarrow 2_{2,1}}$	$a^{(n)}_{\leftarrow 3_{0,3}}$	$a^{(n)}_{\leftarrow 3_{1,2}}$	$a^{(n)}_{\leftarrow 3_{2,1}}$	$a^{(n)}_{\leftarrow 4_{1,4}}$	$a^{(n)}_{\leftarrow 3_{3,0}}$	$a^{(n)}_{\leftarrow 4_{2,3}}$
0	–10.1876	–9.8101	–10.1703	–10.5424	–12.2931	–9.6483	–11.1640	–11.3694	–12.4494
1	6.5796	0.5647	–3.0277	–0.6399	9.2629	–13.2040	–3.0869	–5.0876	–0.7116
2	–22.7661	–5.9239	7.4800	0.5258	–29.2146	36.8854	9.9865	15.9120	6.3499
3	31.4597	9.9441	–9.2544	0.0215	37.5916	–46.7970	–14.0478	–22.1115	–13.6319
4	–15.6234	–5.1116	4.6355	0.0989	–17.6172	22.2593	7.1424	11.2390	8.6836
$1_{1,0}$		$a^{(n)}_{\leftarrow 2_{1,2}}$	$a^{(n)}_{\leftarrow 2_{2,1}}$	$a^{(n)}_{\leftarrow 3_{0,3}}$	$a^{(n)}_{\leftarrow 3_{1,2}}$	$a^{(n)}_{\leftarrow 3_{2,1}}$	$a^{(n)}_{\leftarrow 4_{1,4}}$	$a^{(n)}_{\leftarrow 3_{3,0}}$	$a^{(n)}_{\leftarrow 4_{2,3}}$
0		–10.8118	–9.7732	–11.4567	–10.1456	–10.3113	–11.2115	–10.6512	–11.3165
1		7.4280	–3.1678	5.0975	–5.2141	–9.7549	–3.1187	–6.1335	–5.1081
2		–23.3047	8.0202	–13.7565	12.4640	27.6769	10.0179	18.9963	16.2240
3		30.0489	–10.1443	16.0631	–15.3446	–35.2199	–14.3942	–26.1038	–23.4875
4		–14.0322	5.0836	–6.6633	7.4845	16.6678	7.3682	13.1249	12.3566
$2_{1,2}$			$a^{(n)}_{\leftarrow 2_{2,1}}$	$a^{(n)}_{\leftarrow 3_{0,3}}$	$a^{(n)}_{\leftarrow 3_{1,2}}$	$a^{(n)}_{\leftarrow 3_{2,1}}$	$a^{(n)}_{\leftarrow 4_{1,4}}$	$a^{(n)}_{\leftarrow 3_{3,0}}$	$a^{(n)}_{\leftarrow 4_{2,3}}$
0			–10.1667	–10.2893	–10.2134	–9.8133	–10.3763	–10.6506	–11.6818
1			1.7849	3.5690	0.3910	–6.0796	–4.0238	–6.3023	–0.8441
2			–6.5466	–13.9411	–2.5257	16.9870	11.5290	19.7761	6.2154
3			7.6661	19.5139	2.9383	–22.4136	–16.0531	–28.3573	–12.1634
4			–2.9588	–9.3103	–0.9904	11.1376	8.3618	14.9054	7.5419
$2_{2,1}$				$a^{(n)}_{\leftarrow 3_{0,3}}$	$a^{(n)}_{\leftarrow 3_{1,2}}$	$a^{(n)}_{\leftarrow 3_{2,1}}$	$a^{(n)}_{\leftarrow 4_{1,4}}$	$a^{(n)}_{\leftarrow 3_{3,0}}$	$a^{(n)}_{\leftarrow 4_{2,3}}$
0				–12.5143	–11.3874	–8.9216	–10.5847	–9.9467	–10.4404
1				16.9687	10.5262	–9.3767	–4.1839	–3.8886	–6.4087
2				–48.2815	–34.1153	23.6301	9.8197	12.2989	19.9189
3				56.9744	44.0339	–28.4478	–10.7217	–17.6984	–29.2215
4				–24.2411	–20.4615	13.0161	4.2197	9.2371	15.5988
$3_{0,3}$					$a^{(n)}_{\leftarrow 3_{1,2}}$	$a^{(n)}_{\leftarrow 3_{2,1}}$	$a^{(n)}_{\leftarrow 4_{1,4}}$	$a^{(n)}_{\leftarrow 3_{3,0}}$	$a^{(n)}_{\leftarrow 4_{2,3}}$
0					–10.1031	–10.2176	–9.6188	–12.0621	–10.2604
1					4.4953	–3.6094	–3.9802	1.4928	–4.3320
2					–16.4020	12.8009	10.3903	4.3519	13.7521
3					22.5214	–19.8468	–14.2019	–14.1974	–20.5819
4					–11.0314	10.9007	7.5242	10.0233	11.1931

The discrepancies between our rate coefficients and the Phillips et al. (1996) rate coefficients at 20 K range between 2% and 25%. Phillips et al. (1996) used a smaller basis set, a sparser energy grid and coupled states calculations above 450 cm^{-1}. The various small errors introduced in their calculations sometimes compensate for one another and sometimes add to one another. Therefore the effect on the data is neither homogeneous among different transitions nor among different temperature, and is difficult to predict. Nevertheless it should be noted that the largest differences correspond to the smallest rates. We believe that most of our effective rate coefficients have a maximum error of 3% for all given transitions and temperatures, and for the given potential energy surface. The smallest effective rate coefficients might have a higher error, but these rates are unimportant.

For astrophysical use, our de-excitation effective excitation rate coefficients may be fitted by the analytical form used by Balakrishnan et al. (1999) and used in Paper I (Dubernet & Grosjean 2002):

$$\log_{10} \hat{R}_{j_2=1}(j\alpha \rightarrow j'\alpha')(T) = \sum_{n=0}^{N} a^{(n)}_{j_2=1;j\alpha\rightarrow j'\alpha'} \; x^n \qquad (3)$$

where $x = 1/T^{1/3}$. Tables 4 and 5 give the fitted values of $a_{j_2=1;j\alpha\rightarrow j'\alpha'}$ for the de-excitation effective rate coefficients given in Tables 2 and 3 respectively. The excitation effective rate coefficients can be obtained by detailed balance using the energy levels given by Green et al. (1993). In the present paper our effective rate coefficients follow the detailed balance principle within the calculation error, because there are no transitions to the $j_2 = 3$ rotational level of H_2 at very low energy. But in

Table 5. Coefficients $a^{(n)}_{j_2=1;j\alpha\leftarrow j'\alpha'}$ (n = 0 to 4) of the polynomial fit (Eq. (3)) to the effective de-excitation rate coefficients of para-water in Table 3. The effective excitation rate coefficients can be obtained by detailed balance. The first column gives the final state and the polynomial order n, the following columns give the fitting coefficients for various initial states. The levels are labelled with $j_{K_{-1}K_1}$.We emphasize that these fits are only valid in the temperature range from 5 K to 20 K.

$0_{0,0}$	$a^{(n)}_{\leftarrow 1_{1,1}}$	$a^{(n)}_{\leftarrow 2_{0,2}}$	$a^{(n)}_{\leftarrow 2_{1,1}}$	$a^{(n)}_{\leftarrow 2_{2,0}}$	$a^{(n)}_{\leftarrow 3_{1,3}}$	$a^{(n)}_{\leftarrow 3_{2,2}}$	$a^{(n)}_{\leftarrow 4_{0,4}}$	$a^{(n)}_{\leftarrow 4_{1,3}}$	$a^{(n)}_{\leftarrow 3_{3,1}}$
0	–9.2196	–10.5644	–12.5365	–10.0061	–11.2977	–12.8447	–11.8093	–13.6415	–11.9075
1	–4.8077	0.7471	12.0237	–8.0560	–2.6392	–2.7402	–1.2909	8.9455	–3.8667
2	11.9283	–3.1298	–35.7592	21.1002	7.1789	21.6079	3.4620	–27.4139	11.8491
3	–14.3880	3.7884	42.8885	–25.0268	–9.1812	–42.8813	–5.1317	35.4918	–16.4370
4	6.6227	–1.2576	–18.3335	11.5425	4.7295	26.0394	2.9875	–17.0599	8.5438
$1_{1,1}$		$a^{(n)}_{\leftarrow 2_{0,2}}$	$a^{(n)}_{\leftarrow 2_{1,1}}$	$a^{(n)}_{\leftarrow 2_{2,0}}$	$a^{(n)}_{\leftarrow 3_{1,3}}$	$a^{(n)}_{\leftarrow 3_{2,2}}$	$a^{(n)}_{\leftarrow 4_{0,4}}$	$a^{(n)}_{\leftarrow 4_{1,3}}$	$a^{(n)}_{\leftarrow 3_{3,1}}$
0		–10.7363	–10.2653	–9.6180	–10.4682	–10.7198	–11.4634	–11.8217	–10.8323
1		8.0746	3.6744	–4.8781	–1.8012	–6.4847	0.2937	–1.4055	–4.8412
2		–23.9005	–14.1624	12.0389	4.8826	22.0777	–1.7585	4.6025	14.1863
3		29.1820	19.2240	–13.8634	–6.9287	–32.6194	3.5667	–6.8634	–18.9250
4		–12.8709	–8.9750	6.4187	3.9533	17.1533	–2.2181	3.4001	9.4947
$2_{0,2}$			$a^{(n)}_{\leftarrow 2_{1,1}}$	$a^{(n)}_{\leftarrow 2_{2,0}}$	$a^{(n)}_{\leftarrow 3_{1,3}}$	$a^{(n)}_{\leftarrow 3_{2,2}}$	$a^{(n)}_{\leftarrow 4_{0,4}}$	$a^{(n)}_{\leftarrow 4_{1,3}}$	$a^{(n)}_{\leftarrow 3_{3,1}}$
0			–9.9342	–9.9715	–9.6593	–9.8947	–10.4306	–12.7925	–11.9214
1			3.6405	–4.4341	–2.2514	–6.6853	–3.3175	11.1765	0.9281
2			–14.0091	12.7021	4.0588	21.2566	7.8651	–36.0036	–1.5458
3			20.0353	–15.6973	–5.0059	–31.0300	–9.0122	48.1492	–0.1500
4			–10.0308	7.2244	3.0100	16.2566	4.1399	–23.6727	1.1650
$2_{1,1}$				$a^{(n)}_{\leftarrow 2_{2,0}}$	$a^{(n)}_{\leftarrow 3_{1,3}}$	$a^{(n)}_{\leftarrow 3_{2,2}}$	$a^{(n)}_{\leftarrow 4_{0,4}}$	$a^{(n)}_{\leftarrow 4_{1,3}}$	$a^{(n)}_{\leftarrow 3_{3,1}}$
0				–9.9108	–10.8548	–9.6450	–11.3711	–10.4960	–10.6282
1				1.9280	5.2417	–6.4971	3.0639	–4.6407	–4.4253
2				–8.2382	–16.2733	19.3304	–11.7300	11.9976	12.6545
3				11.5316	20.3823	–27.1327	17.7318	–15.2811	–17.0611
4				–5.3817	–9.0809	13.8905	–9.4384	7.3365	8.7126
$2_{2,0}$					$a^{(n)}_{\leftarrow 3_{1,3}}$	$a^{(n)}_{\leftarrow 3_{2,2}}$	$a^{(n)}_{\leftarrow 4_{0,4}}$	$a^{(n)}_{\leftarrow 4_{1,3}}$	$a^{(n)}_{\leftarrow 3_{3,1}}$
0					–10.8154	–9.5935	–12.7240	–11.3048	–10.0644
1					2.7559	–4.2012	15.0927	1.0408	–2.7224
2					–7.3990	10.5606	–54.6129	–1.1575	8.4156
3					4.4787	–14.5285	81.0160	–0.3876	–12.0942
4					–3.4467	7.3934	-43.1518	0.5005	6.4608

general only the $R(j\alpha, j_2 = 1 \rightarrow j'\alpha', j'_2)$ and the $R(j\alpha \rightarrow j'\alpha')$ satisfy the usual detailed balance relations between forward and reverse rates, and the $\hat{R}_{j_2}(j\alpha \rightarrow j'\alpha')$ do not since they do not involve a complete thermal average (Phillips et al. 1996).

A fourth-order polynomial ($n = 4$) is required to cover the whole range of temperature and to provide a fitting error better than 0.02% on all rate coefficients. We emphasize that these fits are only valid in the temperature range from 5 K to 20 K.

It is interesting to note that the extrapolation method described in the introduction works very well for the present results with ortho dihydrogen. We recall that it does not work well for results with para dihydrogen. It is therefore difficult to judge the precision of an extrapolation procedure before the calculations are actually performed. It raises the question of the required precision of rate coefficients in the modelling of astrophysical media.

3. Application to cold molecular clouds

Motivated by this problem we checked the influence of the precision of the rate coefficients on the predicted line intensities of the ground state transition observed by SWAS (Melnick et al. 2000) at 557 GHz. The predicted intensities were obtained by means of a LVG model to solve self-consistently the non-LTE population equilibrium, and whose details are reported in Ceccarelli et al. (1998, 2002). H_2 densities of 3×10^3 cm^{-3} and 1×10^5 cm^{-3} were used. The results were not very sensitive to the change in density.

We compared the predicted line intensities $I_{\rm cal}^{53}$ and $I_{\rm cal}^{51}$ obtained respectively with the fully converged rate coefficients corresponding to the large basis set $B(5, 3)$, and with the less accurate rate coefficients calculated with a $B(5, 1)$ basis set. We found a maximum difference of 2% in the predicted line intensities, which corresponds to the difference in the corresponding rate coefficients for the $1_{0,1} \rightarrow 1_{1,0}$ transition. We performed extra tests using arbitrary rate coefficients with higher differences and found the same linear effect. More work should be carried out on the subject, but it is not the purpose of the present paper.

4. Conclusion

This paper is a continuation of the work of Dubernet & Grosjean (2002) and of the work of Phillips and co-workers (Green et al. 1993; Phillips et al. 1994, 1995, 1996) on the excitation rates of H_2O by H_2. Phillips et al. (1996) gave excitation rates in the range from 20 K to 140 K; we have calculated these rates in the range from 5 K to 20 K. Unlike Paper I (Dubernet & Grosjean 2002), our improved dynamical calculations confirm the results of Phillips et al. (1996) at 20 K. We have also provided fits of the de-excitation rates that are valid in the range from 5 K to 20 K. The results of the present paper, the excitation rates of other transitions and the associated cross sections will be made available on our web site[1]. We are currently investigating the temperature range up to 1500 K.

We gave a first estimation of the effect of the rate coefficient precision on the water ground transition at 557 GHz observed by SWAS. We found a linear correlation between differences in rate coefficients and differences in predicted line intensities. We hope that this simple test will motivate more general studies on the influence of the rate coefficient precision on predicted quantities extracted from modelling, in particular in the case of the excitation of H_2O. The outcome of such studies would be a very useful guide for calculations of rate coefficients for astrophysical applications.

Acknowledgements. Most scattering calculations were performed at the CINES under project aob2271. This work is supported by the PCMI National Program.

References

Balakrishnan, N., Forrey, R. C., & Dalgarno, A. 1999, ApJ, 514, 520
Ceccarelli, C., Baluteau, J.-P., Walmsley, M., et al. 2002, A&A, 383, 603
Ceccarelli, C., Caux, E., White, G. J., et al. 1998, A&A, 331, 372
Ceccarelli, C., Hollenbach, D. J., & Tielens, A. G. G. M. 1996, ApJ, 471, 400
Doty, S. D., & Neufeld, D. A. 1997, ApJ, 489, 122
Dubernet, M.-L., & Grosjean, A. 2002, A&A, 390, 793
Graff, M. M., & Dalgarno, A. 1987, ApJ, 317, 432
Green, S., Maluendes, S., & McLean, A. D. 1993, ApJS, 85, 181
Hutson, J. M., & Green, S. 1994, MOLSCAT computer code, version 14 (UK: Collaborative Computational Project No. 6 of the Science and Engineering Research Council)
Kaufman, M. J., & Neufeld, D. A. 1996a, ApJ, 456, 611
Kaufman, M. J., & Neufeld, D. A. 1996b, ApJ, 456, 250
Kessler, M. F., Steinz, J. A., Anderegg, M. E., et al. 1996, A&A, 315, L27
Kyrö, E. 1981, J. Mol. Spectrosc., 88, 167
Lee, H.-H., Bettens, R. P. A., & Herbst, E. 1996, A&AS, 119, 111
Melnick, G. J., Stauffer, J. R., Ashby, M. L. N., et al. 2000, ApJ, 539, L77
Phillips, T. R., Maluendes, S., & Green, S. 1995, J. Chem. Phys., 102, 6024
Phillips, T. R., Maluendes, S., & Green, S. 1996, ApJS, 107, 467
Phillips, T. R., Maluendes, S., McLean, A. D., & Green, S. 1994, J. Chem. Phys., 101, 5824
Tielens, A. G. G. M., & Allamandola, L. J. 1987a, in Interstellar Processes, ASSL, 134, 397
Tielens, A. G. G. M., & Allamandola, L. J. 1987b, in Physical Processes in Interstellar Clouds, 333

[1] BASECOL.obs-besancon.fr